Time-Resolved Spectroscopic Studies of B_{12} Coenzymes: The Photolysis of Methylcobalamin Is Wavelength Dependent

Joseph J. Shiang, Larry A. Walker II, Neil A. Anderson, Allwyn G. Cole, and Roseanne J. Sension*

Department of Chemistry, University of Michigan, Ann Arbor, Michigan 48109-1055

Received: July 13, 1999; In Final Form: September 13, 1999

Femtosecond to nanosecond transient absorption spectroscopy has been used to investigate the primary photochemistry of the B_{12} coenzymes, methylcobalamin and 5′-deoxyadenosylcobalamin. Photolysis at excitation wavelengths in the near UV (400 nm) and visible (520−530 nm) are compared. Measurements were performed with femtosecond time resolution covering time delays of up to 9 ns. The photochemistry of methylcobalamin is found to depend strongly on excitation wavelength, while the photochemistry of adenosylcobalamin is essentially wavelength independent over the range studied. Excitation of methylcobalamin at 400 nm results in a partitioning between prompt bond homolysis and formation of a metastable cob(III)-alamin photoproduct as reported earlier [Walker, L. A., II; Jarrett, J. T.; Anderson, N. A.; Pullen, S. H.; Matthews, R. G.; Sension, R. J. *J. Am. Chem. Soc.* **1998**, *120*, 3597−3603]. Excitation of methylcobalamin at 520 nm in the visible $\alpha\beta$-band results only in formation of the metastable cob(III)alamin photoproduct. No prompt bond homolysis is observed. The metastable photoproduct partitions between formation of cob(II)-alamin ($14 \pm 5\%$) and recovery of the methylcobalamin starting material ($86 \pm 5\%$) on a 1.0 ± 0.1 ns time scale. The quantum yield for bond homolysis in methylcobalamin is determined by the wavelength-dependent partitioning between prompt homolysis and formation of the metastable photoproduct and by the partitioning of the metastable photoproduct between bond homolysis and ground-state recovery. In contrast, excitation of adenosylcobalamin at both 400 and 520 nm results in the development of a difference spectrum characteristic of the formation of cob(II)alamin on a picosecond time scale. The quantum yield for bond homolysis in this case is determined primarily by the competition between geminate recombination and diffusion to form solvent-separated radical pairs. The caging fraction for adenosylcobalamin in aqueous solution at room temperature is 0.71 ± 0.05.

Introduction

The photolysis of alkylcobalamins, especially the biologically active B_{12} coenzymes, methylcobalamin and 5′-deoxyadenosylcobalamin, has sometimes been used as a model or experimental substitute for the thermal homolysis of these compounds.[1−6] Recent studies have examined recombination following photolysis under the influence of an external magnetic field as a probe of field effects on the geminate radical pair.[1−3] Photolysis and recombination have also been used as probes of electronic trans-axial ligand effects and of cage effects in a protein environment.[4,5] Photoacoustic measurements have been used to determine bond dissociation energies.[6]

On the other hand, it has been pointed out, quite appropriately, that in order to use photolysis as a model or substitute for thermolysis, the photolysis mechanism must be well understood.[7−9] It has long been known that photolysis of alkylcobalamins under anaerobic conditions results in the homolytic cleavage of the carbon−cobalt bond to form an alkyl radical and a cob(II)alamin radical.[10] Photoinduced homolysis occurs with substantial quantum yields, ranging from 0.1 to 0.5 for 6-coordinate base-on cobalamins.[11−13] Continuous wave measurements with excitation at 442 nm determined photolysis quantum yields of $\varphi = 0.20 \pm 0.03$ for adenosylcobalamin and $\varphi = 0.35 \pm 0.03$ for methylcobalamin.[13] Nanosecond transient absorption measurements on adenosylcobalamin were used to determine a quantum yield of $\varphi = 0.23 \pm 0.04$ following excitation at 532 or 355 nm.[14] To utilize photolysis as an effective tool for the study of B_{12}-dependent enzymes, however, it is necessary to have a more detailed picture of the photolysis mechanism than is afforded by nanosecond to steady-state quantum yields alone. Measurements of photolysis quantum yields, like those of thermolysis yields, average over all accessible dissociation pathways. Time- and wavelength-resolved photolysis studies provide a direct means of examining individual reaction paths in detail.

Recently, we reported femtosecond to nanosecond transient absorption data, demonstrating that excitation of methylcobalamin at 400 nm results in the formation of two distinct photoproducts.[15] These data demonstrated that ca. 27% of the initially excited methylcobalamin molecules undergo bond homolysis, forming methyl radical and cob(II)alamin. The remaining molecules form a metastable photoproduct with an absorption spectrum that is consistent with the formation of a cob(III)alamin species. The observation of a prominent blue-shifted gamma band centered at 340 nm suggests that this metastable photoproduct is a cob(III)alamin species with a very weak axial ligand. The picosecond transient absorption data may be interpreted in terms of heterolytic cleavage of the carbon−cobalt bond to form an ion pair between a five-coordinate cob(III)alamin and a methyl anion or, alternatively, in terms of

* Corresponding author. E-mail: rsension@umich.edu.

10.1021/jp992358r CCC: $18.00
Published on Web 11/04/1999

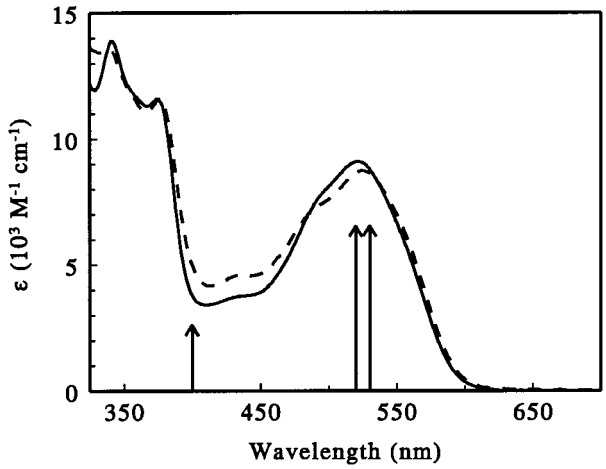

Figure 1. UV−visible absorption spectra of methylcobalamin (solid line) and 5′-deoxyadenosylcobalamin (dashed line). The arrows indicate the pump wavelengths (400, 520, and 530 nm) used in this work.

population trapped in a localized (i.e., ion pair-like) charge transfer state. These results suggest that the quantum yield for photolysis of methylcobalamin is determined, at least in part, by the initial branching ratio for bond homolysis.

A similar transient absorption study of adenosylcobalamin gave distinctively different results.[16] The only well-defined photoproduct spectrum observed following excitation of adenosylcobalamin corresponds to the formation of cob(II)alamin, implying that bond homolysis occurs on a picosecond time scale. Unlike methylcobalamin, the photolysis quantum yield in adenosylcobalamin is determined primarily by competition between geminate recombination and diffusion to form solvent-separated radical pairs.

The 400 nm excitation wavelength used in both of our earlier investigations is technically convenient (the second harmonic of a femtosecond titanium sapphire laser) but is not ideally suited to the study of alkylcobalamins. As illustrated in Figure 1, this wavelength falls in the valley between the visible and ultraviolet (UV) absorption bands, closer to the UV absorption band than to the strong, visible $\alpha\beta$-band. In the present paper we report the results of femtosecond to nanosecond transient absorption measurements following excitation at 520 or 530 nm, near the peak of the visible $\alpha\beta$-absorption band. Comparison of these data with the data reported earlier for 400 nm excitation demonstrates that the photochemistry of adenosylcobalamin is largely independent of excitation wavelength between 400 and 530 nm, while the photochemistry of methylcobalamin is strongly dependent on the excitation wavelength. Different excited states of methylcobalamin have very different photodissociation pathways. In addition to providing data for excitation in the $\alpha\beta$-absorption band, the present study augments our previous work by extending quantitative transient absorption kinetic traces to time delays of 9 ns. These data produce well-defined numbers for the caging fraction of adenosylcobalamin in solution.

Experimental Section

Transient Absorption Measurements. Transient absorption measurements were performed using a femtosecond laser system and experimental method as described previously, with a few important modifications.[15] Briefly, a self-mode-locked titanium sapphire oscillator, running at 100 MHz and producing 20 fs, 2 nJ pulses, was regeneratively amplified at a 1 kHz repetition rate. The resulting laser beam was centered at approximately 800 nm, providing 400 μJ, 70 fs pulses at a repetition rate of 1 kHz. Tunable pump pulses were generated by sending the 800 nm laser pulse into a home-built optical parametric amplifier constructed according to the design of Wilhelm et al.[17] In this amplifier a small portion of the fundamental is used to produce a white light continuum in a 3 mm thick piece of sapphire. The remaining beam is directed through an 0.5 mm β-barium borate (BBO) crystal to generate the second harmonic. Amplification at the desired wavelength is achieved by mixing the continuum with the second harmonic in a second BBO crystal (2 mm). The wavelength may be selected by angle tuning the amplification crystal, or alternatively, for a narrower spectral range, by placing an interference filter in the continuum before the amplification crystal. For the present set of measurements the output consisted of 100−200 fs pulses centered at peak wavelengths between 520 and 530 nm inclusive, with pulse energies of 0.5−1.5 μJ/pulse. For most of the measurements reported here the undoubled fundamental remaining after the initial BBO crystal was directed into a second piece of sapphire, with the resulting white-light continuum providing the probe pulses. Interference filters were used to select the desired wavelength ranges. The 470 nm probe wavelength used for 520 nm pump measurements was generated by directing the fundamental remaining after the initial BBO crystal into a second home-built OPA producing stable, well-collimated probe pulses.

Using these pulses, time-resolved kinetic and spectral measurements were made as described previously.[15] The probe pulses were delayed with respect to the pump pulses by a 1.5 m computer-controlled motorized translation stage (Newport-Klinger). This stage allows measurements to be made with femtosecond resolution (1 μm step size = 6.667 fs of delay) out to a maximum time delay of ca. 10 ns. A second translation stage on the pump arm (0.1 μm step size) was also used at short time delays. Kinetic traces were collected from −10 ps to +9 ns using variable time steps, typically 0.1 ps (−10 to −1 ps), 0.025 ps (−1 to +1 ps), 0.050 ps (1−5 ps), 0.1 ps (5−10 ps), 0.2 ps (10−20 ps), 0.5 ps (20−50 ps), 1 ps (50−100 ps), 2 ps (100−200 ps), 5 ps (200−500 ps), 10 ps (500 ps to 1 ns), 20 ps (1−2 ns), 50 ps (2−9 ns). A series of kinetic traces extending to 9 ns were also collected at probe wavelengths of 470, 520, 560, and 600 nm following excitation with the second harmonic of the laser at 400 nm. The kinetic traces reported earlier were limited to maximum time delays of 900 ps.[15,16] Extending the time delay to 9 ns allows for a more accurate determination of the longest time constants.

Sample Preparation. Methylcobalamin and adenosylcobalamin were obtained from Sigma and used without further purification. The samples were prepared and kept under anaerobic conditions. This was achieved by bubbling argon through double-distilled, deionized water for a minimum of 1 h after, which ca. 2 mM solutions were made. The samples were placed in a reservoir and kept under argon. The solutions were flowed through a 1 mm path length cell with a rate sufficient to refresh the illuminated volume between pulses. The pH of the methylcobalamin sample was 6.9, the pH of the adenosylcobalamin sample was 6.82, and the solutions were not buffered. UV−visible spectra of the samples obtained before and after laser exposure were identical, indicating minimal photoproduct accumulation during the course of an experiment.

Results

Excitation of Adenosylcobalamin. A series of kinetic traces extending to 9 ns were collected at probe wavelengths of 470, 520, 560, and 600 nm following excitation at 400 nm. Another

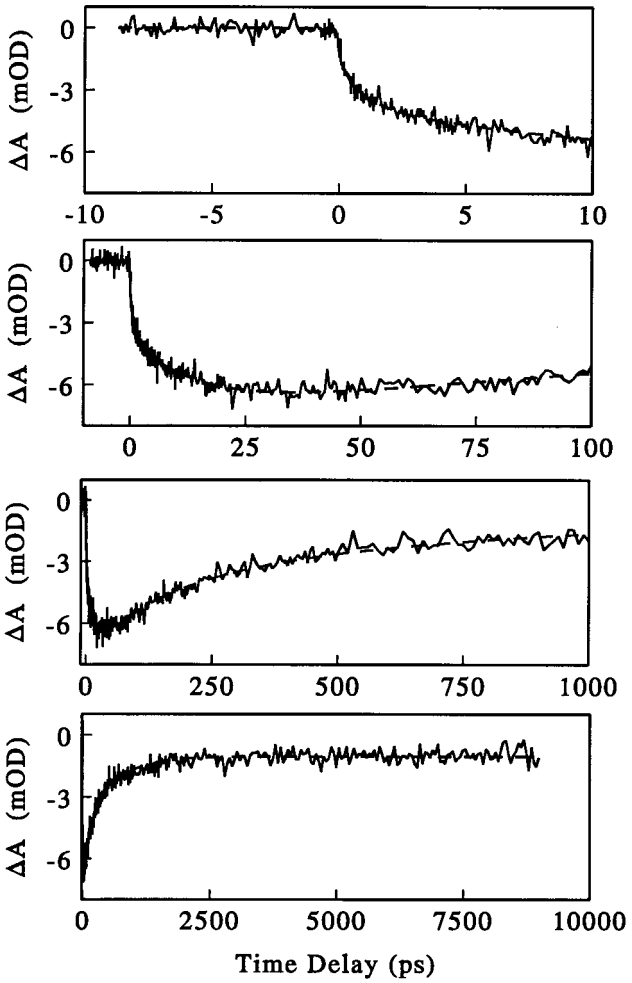

Figure 2. Transient absorption signal obtained at 550 nm following excitation of adenosylcobalamin at 520 nm. The dashed line corresponds to the fit to the data as discussed in the text. The trace is plotted on four different time scales to illustrate the entire temporal response from femtoseconds to nanoseconds.

data set was collected at probe wavelengths of 470, 550, 560, and 600 nm following excitation at 520 nm. A sample trace for 520 nm pump and 550 nm probe is shown in Figure 2. This trace is plotted on four different time scales to illustrate the behavior from femtoseconds (instrument-limited 230 fs rise) out to 9 ns. The early time behavior following excitation at 400 nm is discussed in ref 16. The early time behavior following excitation at 520 nm for additional probe wavelengths is illustrated in plots included in the Supporting Information.

Sample traces obtained for probe wavelengths of 470 and 560 nm following excitation at 400 or 520 nm are compared in Figures 3 and 4 on the nanosecond time scale. The first 100 ps are compared for pump wavelengths of 400 and 520 nm and probe wavelengths of 600, 560, and 470 nm in Figure 5. Subtle wavelength-dependent differences may be observed in the first one or two picoseconds (not resolvable in the figure). However, no significant differences attributable to excitation wavelength are observed after the first one or two picoseconds. A transient difference spectrum obtained 40 ps following the excitation of adenosylcobalamin at 530 nm (data not shown) also indicates the rapid formation of cob(II)alamin. Within the noise of the measurement, the spectrum is identical to that obtained following excitation at 400 nm.[16]

The data obtained with a 400 nm excitation wavelength were fitted by using a global analysis algorithm to a model consisting

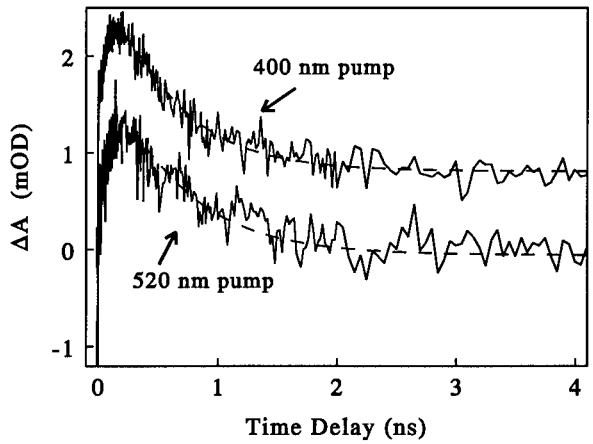

Figure 3. Transient absorption data obtained for adenosylcobalamin with a 470 nm probe wavelength and the pump wavelengths as indicated. The data obtained with a 520 nm pump pulse have been scaled to the peak intensity of the 400 nm trace and offset by −1 mOD for ease of comparison. The dashed line corresponds to the fits to the data as discussed in the text. Note that the rise and decay of the signal are similar for both pump wavelengths.

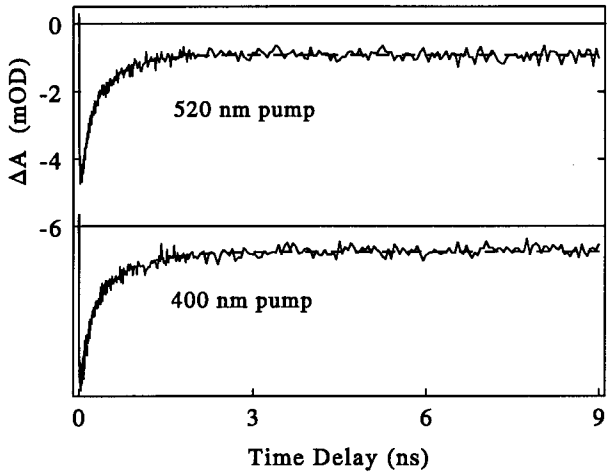

Figure 4. Transient absorption data obtained for adenosylcobalamin with a 560 nm probe wavelength and the pump wavelengths as indicated. The data obtained with a 400 nm pump pulse have been scaled to the peak intensity of the 500 nm trace and offset by −6 mOD for ease of comparison. The dashed line corresponds to the fits to the data as discussed in the text.

of an instrument-limited Gaussian spike, four exponential decay components, and a nondecaying component. The analysis included both the data obtained to 9 ns reported here and the shorter traces reported earlier.[16] The parameters obtained from this analysis are modified only slightly from those reported earlier. The rate constants (time constants in parentheses) obtained for the four exponential components are 0.69 ± 0.05 ps^{-1} (1.4 ps), 0.071 ± 0.005 ps^{-1} (14 ps), 9.5 ± 1.0 ns^{-1} (105 ps), and 1.9 ± 0.2 ns^{-1} (525 ps). The two longer components are determined much more accurately by the present data set than they were by the data reported in our previous paper.

The data obtained with 520 nm excitation were also fitted by using the global analysis routine. In this case, the data required four exponential decay components and a nondecaying component. The parameters obtained from this analysis are consistent with those obtained from the 400 nm data. The rate constants (time constants) obtained for the four exponential components are 1.1 ± 0.2 ps^{-1} (900 fs), 0.071 ± 0.005 ps^{-1} (14 ps), 8.5 ± 0.6 ns^{-1} (118 ps), and 2.1 ± 0.2 ns^{-1} (475 ps).

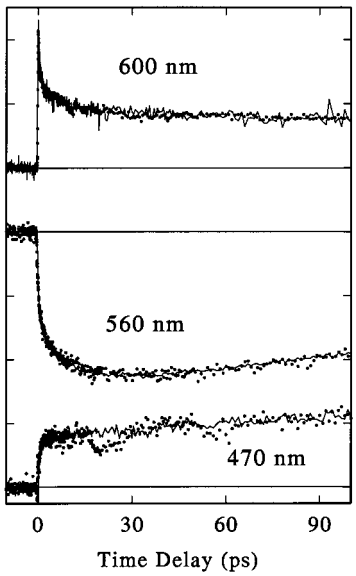

Figure 5. Comparison of transient absorption data obtained for adenosylcobalamin with 400 nm (lines) and 520 nm (points) excitation pulses and the probe wavelengths as indicated. The traces have been offset for clarity. The solid horizontal lines represent zero for each of the three probe wavelengths. Outside of the first one or two picoseconds the traces are independent of excitation wavelength. The initial differences are subtle and are not resolved in this plot.

The dominant decay components observed following excitation of adenosylcobalamin correspond to the geminate recombination of cob(II)alamin and adenosyl radical. The rate constants and amplitudes observed for this geminate recombination component are essentially independent of probe wavelength, demonstrating that cage recombination or escape occurs on a time scale of 500 ± 25 ps.

Excitation of Methylcobalamin. Transient difference spectra were obtained 40 ps, 740 ps, and 2.7 ns following the excitation of methylcobalamin at 530 nm. The spectra obtained for delay times of 40 ps (panel a) and 2.7 ns (panel b) are shown in Figure 6. Comparison of these difference spectra with those observed following excitation at 400 nm (panel c) demonstrate that the photolysis of methylcobalamin is strongly wavelength dependent. The very weak difference spectrum observed 40 ps following excitation at 530 nm is essentially identical to the difference spectrum of the metastable cob(III)alamin species identified following excitation at 400 nm in our previous paper (Figure 7 of ref 15). *No prompt bond homolysis is observed following excitation of methylcobalamin at 530 nm!* The primary photoproduct observed following excitation into the visible absorption band of methylcobalamin at 530 nm is a metastable cob(III)alamin species with a spectrum characteristic of a very weak axial ligand. A difference spectrum characteristic of the formation of cob(II)alamin develops on a nanosecond time scale.

A series of kinetic traces extending to 9 ns were collected at probe wavelengths of 470, 520, and 600 nm following excitation at 400 nm. Another data set was collected at probe wavelengths of 470, 550, 560, and 600 nm following excitation at 520 nm. A transient kinetic trace was also obtained over an 800 ps window for methylcobalamin probed at 558 nm following excitation at 530 nm. A sample trace for 520 nm pump and 550 nm probe is shown in Figure 7. This trace is plotted on four different time scales to illustrate temporal response from femtoseconds to 9 ns. An instrument-limited negative spike is followed by a positive absorption feature that undergoes a multiexponential decay to a long-lived bleach by 9 ns. The early time behavior following excitation at 520 nm for additional

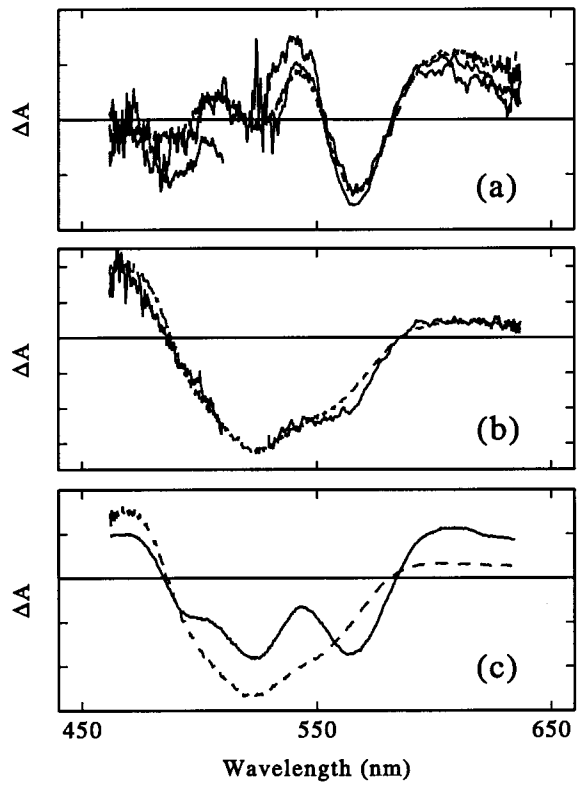

Figure 6. Transient absorption spectra obtained 40 ps (a) and 2.7 ns (b) after excitation of methylcobalamin at 530 nm. The top frame (a) contains two different measurements of the difference spectrum obtained 40 ps after excitation (solid lines) compared with the spectrum of the metastable photoproduct (dashed line) derived from an SVD analysis of the difference spectra obtained following 400 nm excitation (ref 15, Figure 7). The middle frame (b) compares the difference spectrum measured 2.7 nm after excitation (solid line) with the steady-state difference spectrum for the production of cob(II)alamin from methylcobalamin (dashed line). The bottom frame (c) illustrates the difference spectra observed 40 ps (solid line) and 9 ns (dashed line) after excitation with 400 nm pulses. The horizontal lines in each frame correspond to $\Delta A = 0$.

probe wavelengths is illustrated in plots included in the Supporting Information. The early time behavior following excitation at 400 nm is discussed in ref 15. The nanosecond behavior of the data obtained following 400 nm excitation is illustrated in Figure 8, while the nanosecond behavior of data obtained following 520 nm excitation is illustrated in Figure 9. The trace obtained for a 558 nm probe (not shown) starts near zero and exhibits a monotonic increase in the magnitude of the photobleaching over 800 ps.

The data obtained with a 400 nm pump pulse were fitted by using a model consisting of an instrument-limited Gaussian spike, three exponential decay components, and a nondecaying component. The time constants obtained are consistent with those reported previously,[15] with the precision of the longest rate constant improved to 0.93 ± 0.10 ns^{-1} (time constant 1.05 ± 0.10 ns). The kinetic data obtained with a 520 nm pump pulse were fitted by using the same model, yielding rate constants (time constants) of 0.68 ± 0.30 ps^{-1} (1.5 ps), 0.060 ± 0.010 ps^{-1} (17 ps), and 1.10 ± 0.15 ns^{-1} (0.90 ± 0.15 ns). The longest time constant corresponds to the conversion of the difference spectrum from metastable intermediate to cob(II)alamin. This conversion should be independent of excitation wavelength, in agreement with the similar rate constants derived from the data. Combining the two data sets, the lifetime of the photoproduct is found to be 1.0 ± 0.1 ns. The only corrin photoproduct remaining after a few nanoseconds is cob(II)alamin.

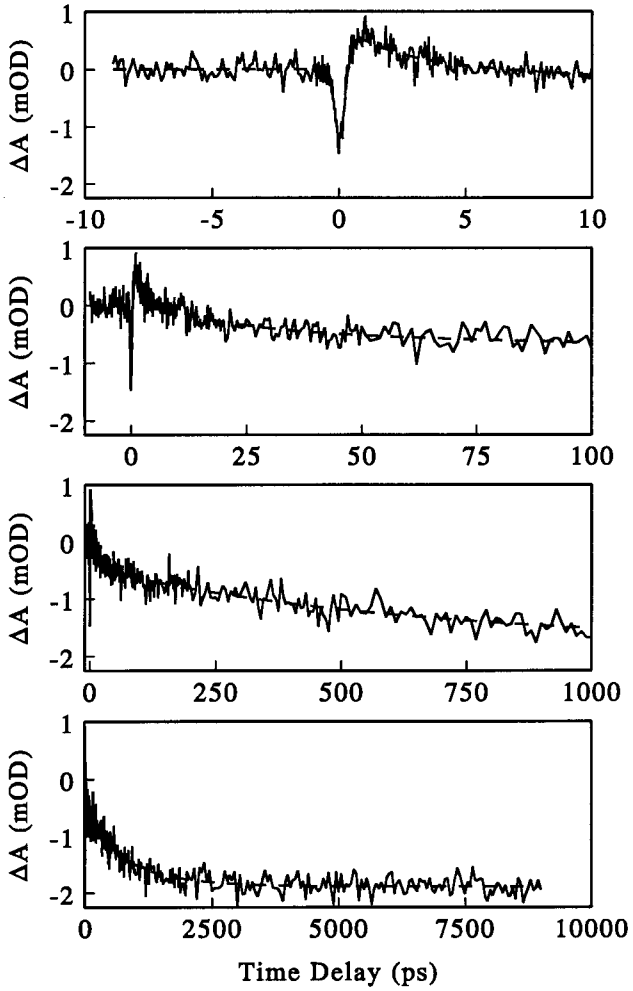

Figure 7. Transient absorption signal obtained at 550 nm following excitation of methylcobalamin at 520 nm. The dashed line corresponds to the fit to the data as discussed in the text. The trace is plotted on four different time scales to illustrate the entire temporal response from femtoseconds to nanoseconds.

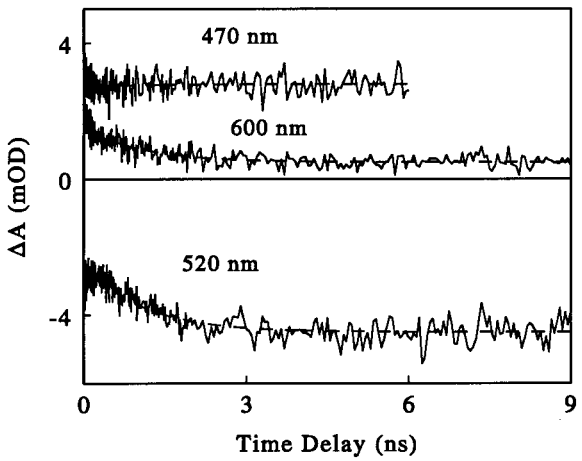

Figure 8. Transient absorption data obtained for methylcobalamin following excitation at 400 nm with the probe wavelengths indicated. The dashed lines correspond to the fits to the data as discussed in the text.

The quantum yield for formation of cob(II)alamin from the metastable intermediate state may be estimated from the position of the isosbestic point observed following 520 nm excitation by using the basis spectra derived in the singular value decomposition (SVD) analysis reported in ref 15. The 558 nm kinetic trace exhibits an increase in the bleaching signal, while the 560 nm kinetic trace exhibits a slight decrease in the bleaching signal on a 1 ns time scale. Taking into account the spectral width of the probe pulses (the interference filters are 10 nm fwhm), this crossing point can be accounted for if the quantum yield for formation of cob(II)alamin is 0.17 (+0.03/−0.05).

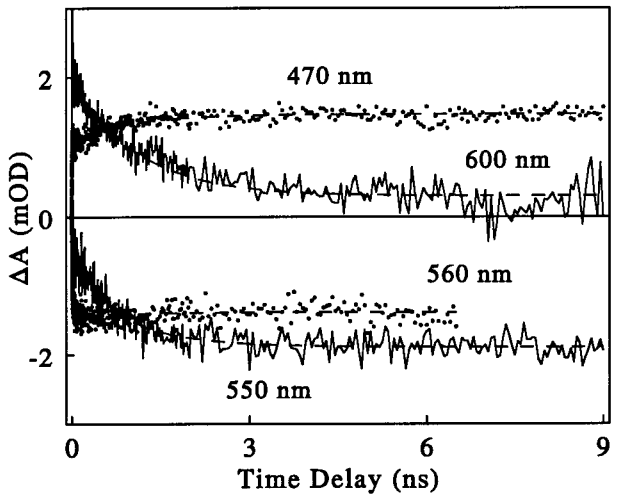

Figure 9. Transient absorption data obtained for methylcobalamin following excitation at 520 nm with the probe wavelengths indicated. The dashed lines correspond to the fits to the data as discussed in the text.

An independent estimate of the quantum yield for the formation of cob(II)alamin from the metastable intermediate may be determined from the data obtained following 400 nm excitation. Measurements reported in ref 15 suggested that $\leq$15% of the metastable photoproduct converts to cob(II)alamin and a methyl radical. This suggestion was based on a slight increase in the population of cob(II)alamin on a 1 ns time scale (see Figure 8 of ref 15). Our ability to verify or quantify this increase was limited by the 150 mm delay stage available for the experiments (1 ns maximum time delay). Those time-resolved difference spectra may now be scaled by using the kinetic traces reported here, extending to a maximum delay time of 9 ns, allowing for a more precise determination of the cob(II)alamin population as a function of time. The spectral and population basis vectors extracted from an SVD analysis of the rescaled data differ only slightly from those reported earlier. The initial partitioning between prompt homolysis (25 $\pm$ 3%) and formation of the metastable photoproduct (75 $\pm$ 3%) is followed by conversion of 12 $\pm$ 2% of the metastable photoproduct to cob(II)alamin. The final quantum yield for bond homolysis at 9 ns is 0.34 $\pm$ 0.04. In the ensuing discussion we will use ca. 14% for the yield of cob(II)alamin from the metastable photoproduct and ca. 86% for the ground-state recovery. These numbers are averages of those obtained from the data sets acquired with 520 and 400 nm pump pulses.

Discussion

Photolysis of Adenosylcobalamin. The data presented above demonstrate that the photochemistry of adenosylcobalamin is independent of excitation wavelength between 400 and 530 nm. A wavelength-independent quantum yield for bond homolysis following excitation of adenosylcobalamin is consistent with earlier reports. Chen and Chance reported a wavelength-independent quantum yield for adenosylcobalamin photolysis (0.20 $\pm$ 0.03 at 442 nm and 0.23 $\pm$ 0.04 at 532 and 355 nm),[13,14] while Taylor et al. reported a quantum yield for adenosylco-

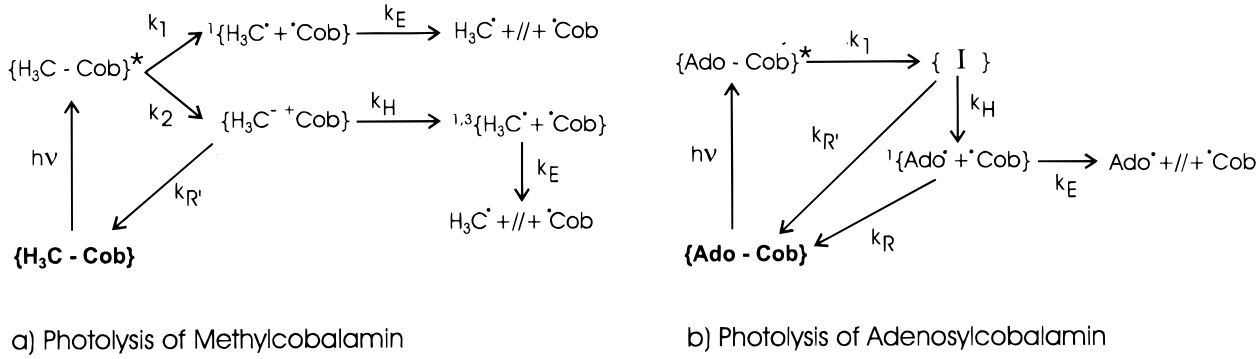

Figure 10. Schematic diagram illustrating the processes observed following the photolysis of methylcobalamin (a) and adenosylcobalamin (b). The symbols R•+//+•Cob represent solvent-separated radical pairs, while brackets around the radicals represent the caged radical pair. The symbol $\{H_3C^{-}\ ^{+}Cob\}$ represents the metastable ion pair-like state formed after excitation of methylcobalamin. For methylcobalamin the rate constants k_1 and k_2 describe the relative formation of geminate radical pairs and the metastable photoproduct, k_E is the rate constant for cage escape, k_H is the rate constant for bond homolysis from the metastable intermediate state, and k_R is the rate constant for ground-state recovery from the metastable state. No geminate recombination is observed for the caged radical pairs. For adenosylcobalamin the rate constant k_1 describes formation of the intermediate or distorted radical pair state, $k_{R'}$ is the rate constant for ground-state recovery from the "I" state, k_H is the rate constant for the formation of the relaxed radical pair, k_R is the rate constant for geminate recombination of the relaxed radical pair, and k_E is the rate constant for escape to form solvent-separated radical pairs. It should be noted that the spin state of the radical pair is not probed in the present set of measurements, and although formation of a singlet radical pair is indicated in the figure, a small yield for the formation of triplet radical pairs is possible.

balamin photolysis that is globally lower (ca. 0.10) but also wavelength independent.[12] Excitation of adenosylcobalamin results in subpicosecond internal conversion to an excited electronic state, presumably the S_1 state, from which bond homolysis occurs.

The simplest model for the photolysis of adenosylcobalamin consistent with the available data is sketched in Figure 10b. In all cases we have assumed that the rate constants for the reverse reactions are much less than the rate constants for the forward reactions. Photolysis of adenosylcobalamin at either 400 or 520−530 nm results in the formation of an intermediate state designated "I" in Figure 10. Two fast components are observed in the transient absorption data, one on a 1−1.4 ps time scale and one on a 14 ps time scale. These two time constants may be related to the formation (1.4 ps) and vibrational relaxation (14 ps) of "I" or to the formation of an electronically excited state (1.4 ps) on the pathway to the formation of "I" (14 ps). This intermediate state decays to form relaxed radical pairs (adenosyl + cob(II)alamin) on a 110 ps time scale.

The spectrum of "I" is similar to that expected for a cob(II)alamin species (see Figure 9 of ref 16). Formation of "I" may correspond to bond homolysis followed by relaxation of the corrin ring structure, as we suggested earlier.[16] Alternatively, "I" may correspond to population trapped in an excited state with a very weak C−Co bond, resulting in a cob(II)alamin-like spectrum. In the former case, photoinduced bond homolysis results in the formation of a geminate radical pair on a time scale less than or equal to 14 ps ($k_1 \geq 0.071$ ps^{-1}), in the latter case photoinduced bond homolysis results in the formation of a geminate radical pair on a time scale of ca. 110 ps ($k_1 = 9$ ns^{-1}). In either case, photoinduced bond homolysis is sufficiently rapid to be a useful technique in the study of the enzyme mechanism and radical dynamics in adenosylcobalamin-dependent enzymes.

Two quantities of importance in thermal as well as photoinduced bond homolysis of adenosylcobalamin are the caging fraction, F_c, and the rate constant for pseudo-unimolecular recombination of caged or geminate radical pairs. The transient absorption data provide a good estimate for both of these quantities. The caging fraction may be calculated from the measured rate constants and from the relative amplitudes of the nondecaying and 500 ps components using rate equations based on the model sketched in Figure 10b. The caging fraction is given by

$$F_c = \frac{k_R}{k_E + k_R} = \frac{1}{1 + QR} \tag{1}$$

where k_R and k_E are defined in Figure 10b, Q is the ratio of rate constants

$$Q = \frac{k_1 k_2}{(k_2 - k_3)(k_1 - k_3)} \tag{2}$$

k_1 is defined in Figure 10b, $k_3 = k_R + k_E$, $k_2 = k_{R'} + k_H$, and R is the ratio of the amplitude of the permanent component to the amplitude associated with the 500 ps decay. In aqueous solution at room temperature ($T \approx 293$ K), the caging fraction, F_c, is 0.71 ± 0.05 and the rate of "unimolecular" cage recombination is $k_R = F_c k_3 = 1.4$ ns^{-1}.

The fraction of "relaxed" radical pairs escaping the cage, $F_{esc} = 1 - F_c = 0.29$, is somewhat larger than the ultimate photolysis yield (0.24 ± 0.04) because a percentage of the molecules in the intermediate "I" state return to the adenosylcobalamin ground state, resulting in a quantum yield for formation of the "relaxed" radical pair state (ϕ_{rrp}) that is less than unity. Our best estimate is $\varphi_{rrp} = 0.85$ for formation of the "relaxed" radical pair state. Approximately 15% of the molecules in the "I" state return to the ground state prior to formation of the "relaxed" radical pair state. Given $k_2 = 9$ ns^{-1} (using the average of the visible and UV rate constants as the best estimate), this implies that the rate constant for recovery from the intermediate "I" state is $k_{R'} = k_2(1 - \varphi_{rrp}) = 1.5$ ns^{-1}. This rate constant is essentially identical to the rate constant for geminate recombination of "relaxed" radical pairs, providing support for our hypothesis that the transition from the "I" state to the "relaxed" state reflects conformational relaxation of the corrin ring.

Photolysis of Methylcobalamin. The spectral changes reported above following visible excitation of methylcobalamin are at variance with the interpretation of earlier measurements. Both Endicott and Netzel[18] and Lott et al.[2] reported an absorption increase at 474 nm and inferred rapid formation of a spectrum characteristic of cob(II)alamin following excitation

with 6 ps pulses at 527 nm[18] or 30 ps pulses at 532 nm.[2] The data presented here are consistent with a nearly constant absorption at 470 nm (Figure 9) but indicate development of a spectrum characteristic of cob(II)alamin on a 1 ns time scale (Figure 6). The kinetic behavior of the absorption signal around 470 nm is singularly uninformative in this particular case. Analysis of the spectral evolution throughout a much larger spectral region is required for a proper interpretation of the dynamics.

The wavelength-dependent quantum yields for bond homolysis deduced from the present data (ca. 0.14 at 520 nm, ca. 0.34 at 400 nm) are consistent with data reported by Taylor et al. for methylcobalamin photolysis.[12] Photolysis quantum yields of ca. 0.28−0.30 from 400 to 450 nm and ca. 0.17 from 510 to 550 nm are reported in ref 12. In a more recent study, Chen and Chance reported a 0.35 ± 0.04 quantum yield for the photolysis of methylcobalamin using continuous excitation at 442 nm,[13] in good agreement with our 400 nm measurements.

The simplest model for the photolysis of methylcobalamin consistent with the available data is sketched in Figure 10a. In all cases we have assumed that the rate constants for the reverse reactions are much less than the rate constants for the forward reactions. The incident photon produces an excited electronic state that either undergoes prompt bond homolysis or forms a metastable intermediate state. Excitation at 520−530 nm results in the formation of this metastable state with 100% yield. Excitation at 400 nm results in 25% prompt bond homolysis and 75% formation of the metastable state. The spectrum of the intermediate state is consistent with heterolytic cleavage of the carbon−cobalt bond to form an ion pair between a five-coordinate cob(III)alamin and a methyl anion. Alternatively, the data may be interpreted in terms of population trapped in a localized (i.e., ion pair-like) charge transfer state, where the bond is not cleaved. Photolysis in an anaerobic environment does not result in the formation of any permanent cob(III)alamin photoproduct, indicating that solvent-separated ion pairs are not formed.

The partitioning at 400 nm may result from direct excitation of two (or more) excited states with one state undergoing direct bond homolysis while the other state results in the formation of the long-lived intermediate. In this case, the quantum yield for prompt homolysis will be related to the relative Franck−Condon factors for the different states at the excitation wavelength. Alternatively, the partitioning may result from competition between bond cleavage and internal conversion following excitation of each excited electronic state.

Regardless of excitation wavelength, approximately 14% of the population of the intermediate state undergoes bond homolysis to form a caged, or geminate, radical pair, while the remaining 86% converts back to methylcobalamin in the ground electronic state. From fits to the experimental data we can assign $k_3 = k_{R'} + k_H = 1.0 \pm 0.1\ ns^{-1}$. The rate constants k_1 and k_2 are greater than $0.05\ ps^{-1}$, with the difference spectra corresponding to cob(II)alamin and/or the metastable photoproduct well developed by 40 ps. No evidence for the geminate recombination of the methyl radical with cob(II)alamin is observed in the time-resolved kinetic traces.

The caging fraction and the rate constant for pseudo-unimolecular recombination of caged or geminate radical pairs are also quantities of importance for the study of thermal and photoinduced bond homolysis of methylcobalamin. Following photolysis of methylcobalamin at 400 nm there is no evidence for recombination of the promptly formed geminate radical pairs, from which we infer that $F_{c,m} \approx 0$ and $k_E \gg k_R$. This observation is in agreement with the small size of the methyl radical, which will facilitate rapid diffusion out of the solvent cage. On the basis of the relative volumes of the radicals (approximately 11:1) and assuming that the rate constant for cage escape is proportional to the diffusion coefficient and thus inversely proportional to the volume, we expect that k_E for the methyl radical will be $\geq 6.6\ ns^{-1}$ compared with ca. $0.6\ ns^{-1}$ ($k_E = k_3 - k_R$) observed for the adenosyl radical. The methyl radical should escape the solvent cage on a time scale ≤150 ps. If the "unimolecular" rate constants for the cage recombination of the methyl radical and adenosyl radical with cob(II)alamin are similar, the caging fraction for methylcobalamin is estimated at $F_{c,m} \leq 1.4\ ns^{-1}/(1.4\ ns^{-1} + 6.6\ ns^{-1}) \leq 0.175$. This estimate provides an upper limit for the methylcobalamin caging fraction in aqueous solution near room temperature. The transient absorption data suggest that the caging fraction is actually closer to zero.

Finally, it should be noted that the wavelength dependence observed for methylcobalamin may provide a reconciliation for conflicting reports in the literature, suggesting the photolysis arises from either a singlet or triplet state producing either a singlet or triplet radical pair.[19,20] The photoinduced bond homolysis of adenosylcobalamin should form predominantly singlet radical pairs as evidenced by the rate of homolysis (bond cleavage occurs with a rate constant no less than $9\ ns^{-1}$ and more likely 0.7 to $0.07\ ps^{-1}$) and by the rapid, efficient, geminate recombination ($k_R = 1.4\ ns^{-1}$). It should be noted, however, that the spin state of the radical pair is not probed in the present set of measurements, and a small yield for the formation of triplet radical pairs is possible. Ethyl- and *n*-propylcobalamin also undergo a rapid wavelength-independent (400−520 nm) photoinduced bond homolysis, producing radical pairs predominantly in the singlet state.[21]

On the other hand, excitation of methylcobalamin may result in bond homolysis following intersystem crossing from the long-lived intermediate state, thereby producing a triplet radical pair. The prompt bond homolysis component observed with near-UV (400 nm) excitation will result in the formation of singlet radical pairs. Excitation in this region may therefore produce a mixture of singlet (prompt) and triplet (delayed) radical pairs. However, the long lifetime of the intermediate state need not signify intersystem crossing and triplet formation. It is also possible that the slow nonradiative relaxation reflects a nanosecond charge recombination process or a simple singlet-state barrier crossing process, with most of the radical pairs produced in the singlet state. The spin state of the radical pair is not probed in the present set of measurements. Future experiments and calculations will be designed to address and answer these questions on the photolysis mechanism.

Conclusions

In this paper we have reported the results of femtosecond to nanosecond transient absorption studies of the primary photochemistry of the B_{12} coenzymes, methylcobalamin and 5′-deoxyadenosylcobalamin. The photochemistry of methylcobalamin is found to depend strongly on the excitation wavelength, while the photochemistry of adenosylcobalamin is essentially wavelength independent over the range studied (400−530 nm). Excitation of methylcobalamin at 400 nm results in a partitioning between prompt bond homolysis and formation of a metastable cob(III)alamin photoproduct as reported earlier.[15] Excitation of methylcobalamin in the visible $\alpha\beta$-band results only in formation of the metastable cob(III)alamin photoproduct. No prompt bond homolysis is observed. The metastable photoproduct partitions

between formation of cob(II) alamin (14 ± 5%) and recovery of the methylcobalamin starting material (86 ± 5%) on a 1.0 ± 0.1 ns time scale. The quantum yield for bond homolysis in methylcobalamin is determined by the wavelength-dependent partitioning between prompt homolysis and formation of the metastable photoproduct and by the partitioning of the metastable photoproduct between bond homolysis and ground-state recovery.

Excitation of adenosylcobalamin at 400 or 520 nm results in the development of a difference spectrum characteristic of the formation of cob(II)alamin on a picosecond time scale. In this case, the quantum yield for bond homolysis is determined primarily by the competition between geminate recombination and diffusion to form solvent-separated radical pairs. In aqueous solution at room temperature ($T \approx 293$ K), the caging fraction following homolysis of adenosylcobalamin is 0.71 ± 0.05 and the rate constant for "unimolecular" cage recombination is $k_R = 1.4$ ns^{-1} ($\tau_R = 710$ ps).

Acknowledgment. This project is supported by NIH grant DK53842. N.A.A. and J.J.S. (in part) are supported by the Center for Ultrafast Optical Science NSF STC PHY 8920108. We would also like to thank Professor Rowena Matthews for enlightening discussions and Ms. Patricia Walker for assistance with some of the measurements reported here.

Supporting Information Available: Transient absorption kinetic traces probed at 600, 560, and 470 nm following 520 nm excitation of methylcobalamin and adenosylcobalamin are included in Supporting Information. The data are plotted to illustrate the early time femtosecond and picosecond behavior. This information is available free of charge via the Internet at http://pubs.acs.org.

Note Added in Proof. While this paper was in press, the work of Kunkely and Vogler on the wavelength-dependent photolysis of methylcobalamin was brought to our attention.[22] This paper also reports a decrease of slightly more than a factor of 2 for the aerobic CW photolysis of methylcobalamin at 546 and 577 nm when compared with photolysis at $\lambda \leq 436$ nm.

References and Notes

(1) Chagovetz, A. M.; Grissom, C. B. *J. Am. Chem. Soc.* **1993**, *115*, 12152−12157.
(2) Lott, W. B.; Chagovetz, A. M.; Grissom, C. B. *J. Am. Chem. Soc.* **1995**, *117*, 12194−12201.
(3) Kruppa, A. I.; Taraban, M. B.; Leshina, T. V.; Natarajan, E.; Grissom, C. B. *Inorg. Chem.* **1997**, *36*, 758−759.
(4) Jarrett, J. T.; Amaratunga, M.; Drennan, C. L.; Scholten, J. D.; Sands, R. H.; Ludwig, M. L.; Matthews, R. G. *Biochemistry* **1996**, *35*, 2464−2475.
(5) Jarrett, J. T.; Drennan, C. L.; Amaratunga, M.; Scholten, J. D.; Ludwig, M. L.; Matthews, R. G. *Bioorg. Med. Chem.* **1996**, *4*, 1237−1246.
(6) Hung, R. R.; Grabowski, J. J. *J. Am. Chem. Soc.* **1999**, *121*, 1359−1364.
(7) Garr, C. D.; Finke, R. G. *J. Am. Chem. Soc.* **1992**, *114*, 10440−10445.
(8) Gerards, L. E. H.; Bulthuis, H.; de Bolster, M. W. G.; Balt, S. *Inorg. Chim. Acta* **1991**, *190*, 47−53.
(9) Koenig, T. W.; Hay, B. P.; Finke, R. G. *Polyhedron* **1988**, *7*, 1499−1516.
(10) Hogenkamp, H. P. C. In *B_{12}*; Dolphin, D., Ed.; John Wiley and Sons: New York, 1982; Vol. 1, pp 295−323.
(11) Pratt, J. M.; Whitear, B. R. D. *J. Chem. Soc A* **1971**, 252−255.
(12) Taylor, R. T.; Smucker, L.; Hanna, M. L.; Gill, J. *Arch. Biochem.* **1973**, 521−533.
(13) Chen, E.; Chance, M. R. *Biochemistry* **1993**, *32*, 1480−1487.
(14) Chen, E.; Chance, M. R. *J. Biol. Chem.* **1990**, *265*, 12987−12994.
(15) Walker, L. A., II; Jarrett, J. T.; Anderson, N. A.; Pullen, S. H.; Matthews, R. G.; Sension, R. J. *J. Am. Chem. Soc.* **1998**, *120*, 3597−3603.
(16) Walker, L. A., II; Shiang, J. J.; Anderson, N. A.; Pullen, S. H.; Sension, R. J. *J. Am. Chem. Soc.* **1998**, *120*, 7286−7292.
(17) Wilhelm, T.; Piel, J.; Riedle, E. *Opt. Lett.* **1997**, *22*, 1494−1496.
(18) Endicott, J. F.; Netzel, T. L. *J. Am. Chem. Soc.* **1979**, *101*, 4000−4002.
(19) Sakaguchi, Y.; Hayashi, H.; I'Haya, Y. J. *J. Phys. Chem.* **1990**, *94*, 291−293.
(20) Rao, D. N. R.; Symons, M. C. R, *J. Chem. Soc., Chem. Commun.* **1982**, 954−955.
(21) Walker, L. A.. II; Shiang, J. J.; Anderson, N. A.; Cole, A. G.; Sension, R. J. Manuscript in preparation.
(22) Kunkely, H.; Vogler, A. *J. Organomet. Chem.* **1993**, *453*, 269−272.